

# LIQUID-LIQUID EXTRACTION RATE OF COAL TAR ABSORPTION OIL IN A CONTINUOUS COUNTERCURRENT SPRAY COLUMN

Student Number: 07M18119

Name: Toshiya MASUDA

Supervisor: Ryuichi EGASHIRA

## 連続式向流接触スプレー塔におけるコールタール吸収油の液液抽出速度 増田 敏也

含窒素複素環式化合物、同素環式化合物、などの有用成分を含むコールタール吸収油を原料分散相、メタノール水溶液を溶媒連続相として、これらを向流接触させた。他の成分に比較して含窒素成分は選択的に溶媒相に抽出され、これらの成分間の分離が可能であることを確認した。含窒素複素環式化合物の収率、その他の成分に対する分離の選択度は、それぞれ最大で 0.5、20 程度であった。総括物質移動容量係数を求め、物質移動係数の相関関係を導き既往の研究と比較し抽出速度過程を検討した。

### 1. Introduction

Coal tar, one of the byproducts from coal carbonization, contains many useful compounds to chemical industry. Absorption oil (AO) which is one of the fractions of coal tar (b.p.=470~550K) contains nitrogen heterocyclic compounds (nitrogen compounds) such as quinoline (Q), isoquinoline (IQ), indole (IL), etc., homocyclic compounds such as naphthalene (N), 1-methylnaphthalene (1MN), 2-methylnaphthalene (2MN), biphenyl (BP), etc., and oxygen heterocyclic compounds such as dibenzofuran (DBF), etc. Generally, the separation and purification of these compounds in AO are carried out in two steps; 1: AO is separated into several fractions by reactive extraction with acid and/or base, 2: these fractions are separated and purified into respective products by distillation, crystallization, adsorption, etc. However, this process is relatively costly because the acid and base used as solvent are very difficult to be recovered and cause corrosion of the equipments. For this problem, the ordinary solvent extraction method with aqueous methanolic solution (MeOH aq.) and the liquid membrane method have been studied<sup>1-6)</sup>. In the continuous countercurrent liquid-liquid extraction<sup>6)</sup>, a spray column was chosen for the equipment, because it was the simplest differential-contact device in laboratory studies, and mass transfer rate was measured and examined.

Mass transfer occurs in three steps which are drop formation, drop coalescence and drop falling. The mass transfer from the single drop during its falling to the continuous phase has been studied<sup>7,8)</sup>. Some researchers<sup>7,8)</sup> correlated the continuous mass transfer coefficient by using  $N_{Re}$ ,  $N_{Sc}$  and  $N_{Sh}$ .

In this study, a countercurrent spray column was applied to the extraction of AO and the separation performance was examined. The mass transfer coefficients were experimentally measured and compared with the previous correlations<sup>7,8)</sup>.

### 2. Experimental

#### 2.1. Apparatus

The schematic diagram of the apparatus is shown in Fig.1. Iwaki Magnet Gear Pumps are equipped with each tank to supply the column with each phase. The column is made of pyrex glass of which the inner diameter is 0.0037m and effective height is 0.495m. Figure 2 shows

the details of the distributors. The distributor of the dispersed phase has 8 needle nozzles of which the inner diameter is  $6 \times 10^{-4}$ m. The distributor of the continuous phase has outlets on side of the cylinder to prevent from falling drops entering in it.

#### 2.2. Procedure

AO and MeOH aq. were stocked in the tanks. AO, dispersed phase, was fed to the top of the column, MeOH aq., continuous phase, to the bottom and these two phases contacted countercurrently. The inlet flow rates were kept constant by controlling the flow valves and the level of the interface between the continuous phase and accumulated raffinate phase at the bottom was maintained by adjusting the drain valve of raffinate phase. The inlet and outlet flow rates were determined by weighing the mass collected in 10 minutes. The holdup of the dispersed phase in the column was determined by measuring the rise of the interface after about 1hour

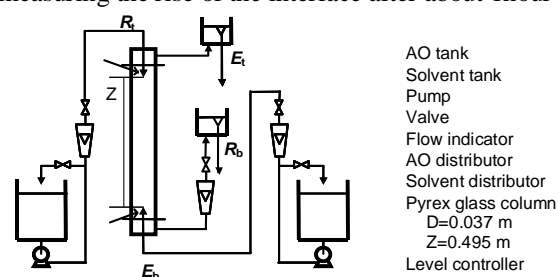


Fig.1 Schematic diagram of the experimental apparatus

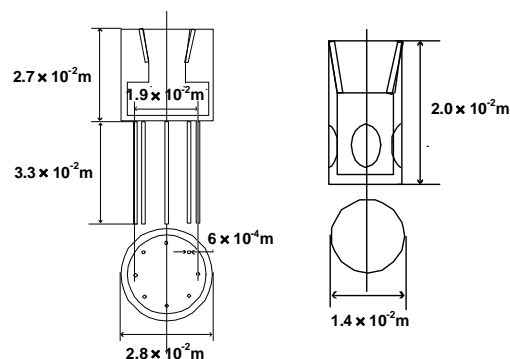


Fig. 2 Details of distributors;

from closing AO inlet and drain at the same time. Each operation was carried out in 3 hours to reach steady state. Each phase was analyzed by GC-2010 (Shimadzu Corp.) The dispersed drop diameters were determined by taking photos of column and measuring the sizes of the drops. **Table 1** shows the principle experimental conditions. The density and viscosity of each phase were measured with pycnometers and Ostwald viscometers.

**Table 1** Experimental condition

No.	feed: AO		solvent: MeOH aq.	
	$R_t$ [ $\text{kg} \cdot \text{m}^{-2} \cdot \text{h}^{-1}$ ]	$y_{\text{MeOH,b}}$ [-]	$E_b$ [ $\text{kg} \cdot \text{m}^{-2} \cdot \text{h}^{-1}$ ]	
EC1	500 ~ 2500	$0.73 \pm 0.03$	$1600 \pm 100$	
EC2	500 ~ 2500	$0.73 \pm 0.03$	$3200 \pm 100$	

### 3. Result and discussion

#### 3.1. Composition of absorption oil

**Table 2** shows the compositions of feed AO. The compositions of the feed AO changed every runs, because the raffinate phase in the previous run was recovered and used as feed in the next run. If necessary, fresh AO was added to the recovered raffinate phase. The ranges of compositions of nitrogen compounds were large, because the transferred amounts to continuous phase were high.

**Table 2** Compositions of feed AO

component $i$	mass fraction, $x_{i,t}$ [-]
Quinoline, Q	0.025~0.071
Isoquinoline, IQ	0.007~0.020
Indole, IL	0.017~0.036
Naphthalene, N	0.025~0.030
1-Methylnaphthalene, 1MN	0.093~0.103
2-Methylnaphthalene, 2MN	0.230~0.254
Biphenyl, BP	0.064~0.072
Dibenzofran, DBF	0.105~0.125
Methanol, MeOH	0~0.012

#### 3.2. Operability

##### 3.2.1. Density and viscosity

**Table 3** shows the densities and viscosities of the materials. The density of the dispersed phase was larger than that of the continuous phase. The viscosities of MeOH aq. and the extract phase were same.

**Table 3** Densities and viscosities of materials

materials	density [ $\text{kg} \cdot \text{m}^{-3}$ ]	viscosity [cP] at 290K
Absorption oil	1040~1100	-
Aqueous methanolic solution	870	1.533
Raffinate phase	1100	-
Extract phase	885~890	1.533

##### 3.2.2. Behavior in the column

In all runs, entrainment of the dispersed phase drops into the continuous phase and flooding were not observed. The substantial mass transfers of these compounds could be detected with this bench scale column of which effective contact height was 0.495m. In the range of higher  $R_t$ , the drops were falling down with zig-zag movement and the coalescence of the dispersed phase and axial mixing were observed.

**Figure 3** shows the results of the holdup of dispersed phase in the column,  $H$ .  $H$  increased with  $R_t$ . **Figure 4** shows the results of the drop diameter,  $d_p$ .  $d_p$  decreased with an increase in  $R_t$ . Specific interfacial area,  $a$ , was

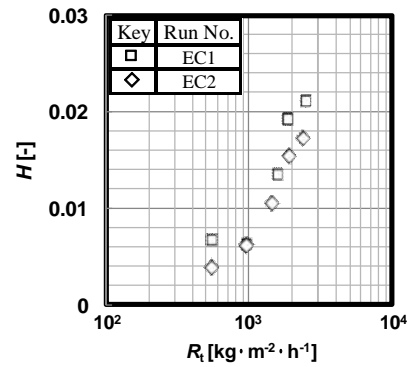


**Fig.3** Holdup of dispersed phase

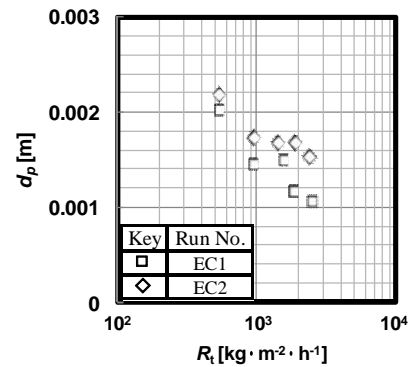


**Fig.4** Drop diameter of dispersed phase

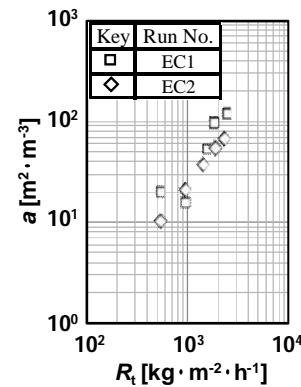


**Fig.5** Specific interfacial area

calculated by,

$$a = 6H/d_p \quad (3.1)$$

**Figure 5** shows the results of  $a$ .  $a$  increased with  $R_t$  and decreased slightly with an increase  $E_b$ .

#### 3.3. Separability

##### 3.3.1. Composition of extract phase

**Figure 6** shows the result of compositions in the extract phase,  $y_{i,t}$ .  $y_{i,t}$  of nitrogen compounds were higher than those of other compounds. In the range of  $R_t < 1500$ ,  $y_{i,t}$  of nitrogen compounds increased with  $R_t$ , and in the range of  $R_t > 1500$ , the changes of  $y_{i,t}$  were small. This was because  $y_{i,t}$  of nitrogen compounds reached equilibrium compositions in the range of  $R_t > 1500$ .  $y_{i,t}$ s of other compounds were almost constant against  $R_t$  because those reached equilibrium compositions.

##### 3.3.2. Yield

Yield of component  $i$ ,  $Y_i$ , was defined as

$$Y_i = E_t \cdot y_{i,t} / (R_t \cdot x_{i,t}) \quad (3.2)$$

**Figure 7** shows the results of  $Y_i$ .  $Y_i$  decreased with an increase in  $R_t$ .  $y_{i,t}$  increased with  $R_t$  and  $y_{i,t}$  almost approached  $y_{i,t}^*$ . However,  $R_t$  became bigger than the

Key	Run No.	i	Key	Run No.	i	Key	Run No.	i	Key	Run No.	i
◆	EC1	Q	▣	EC1	IL	▶	EC1	1MN	▣	EC1	BP
◆	EC2		▣	EC2		▶	EC2		▣	EC2	
▲	EC1	IQ	◆	EC1	N	▣	EC1	2MN	◆	EC1	DBF
▲	EC2		◆	EC2		▣	EC2		◆	EC2	

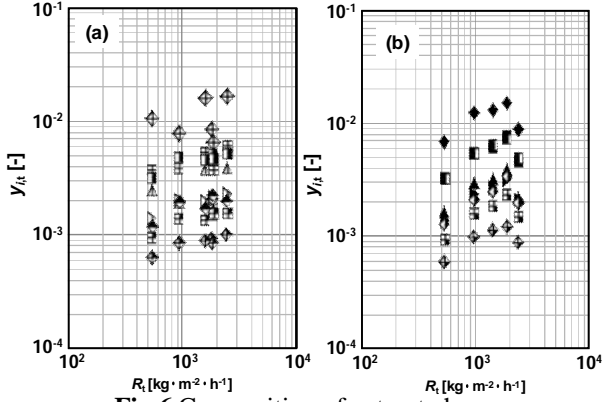


**Fig.6** Composition of extract phase  
(a) in EC1, (b) in EC2

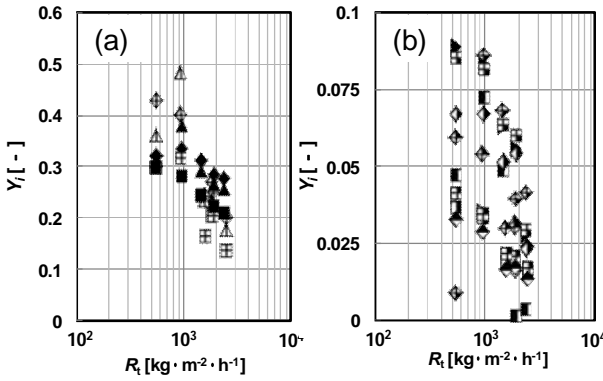


**Fig.7** Yield  
(a) nitrogen compounds, (b) other compounds  
(keys are the same as Fig.6)

increase of the transferred amount of these components.  $Y_i$  slightly increased with  $E_b$ . The maximum  $Y_i$  values of nitrogen compounds and other compounds were 0.5 and 0.1.

### 3.3.3. Separation selectivity

The separation selectivity of component  $i$  relative to 2MN,  $\beta_{i/2MN}$ , was defined as

$$\beta_{i/2MN} = (y_{i,t}/y_{2MN,t}) / (x_{i,b}/x_{2MN,b}) \quad (3.3)$$

**Figure 8** shows the results of  $\beta_{i/2MN}$ .  $\beta_{i/2MN}$  did not change so much as  $R_t$  changed.  $\beta_{i/2MN}$  of nitrogen compounds and other compounds were around 15 and 1. This was because the difference between the distribution coefficients of nitrogen compounds and other compounds was about 10 times. Therefore, the distribution coefficients affected  $\beta_{i/2MN}$ .

## 3.4. Mass transfer rate

### 3.4.1. Overall mass transfer coefficient

The overall mass transfer coefficient based on the continuous phase concentration,  $K_{c,i}$ , was calculated by,

$$d(E \cdot y_i)/dz = -K_{c,i} \cdot a \cdot (y_i^* - y_i) \quad (3.4)$$

The equilibrium composition,  $y_i^*$ , was calculated by,

$$y_i^* = m_i \cdot x_i \quad (3.5)$$

where  $m_i$  ( $=y_{i,1}/x_{i,1}$ ) was distribution coefficient and the value estimated in previous<sup>6)</sup> study was used. **Figure 9** shows the results of  $K_{c,i}$ . In the range of  $R_t < 1500$ ,  $K_{c,i}$

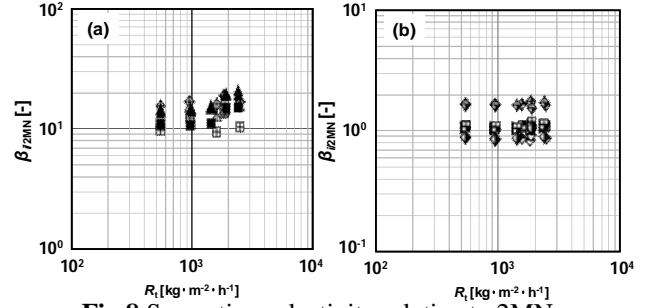


**Fig.8** Separation selectivity relative to 2MN  
(a) nitrogen compounds, (b) other compounds  
(keys are the same as Fig.6)

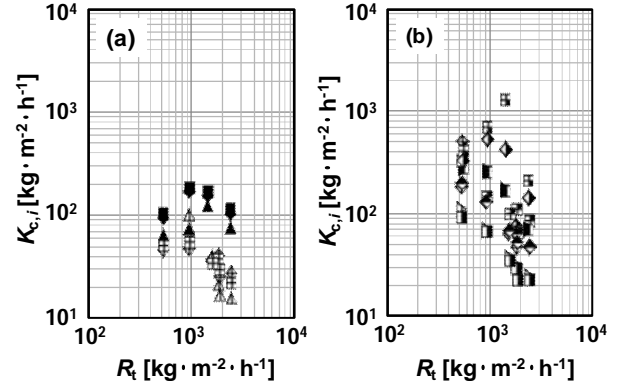


**Fig.9** Overall mass transfer coefficient based on continuous phase concentration  
(a) nitrogen compounds, (b) other compounds  
(keys are the same as Fig.6)

did not change so much, and in the range of  $R_t > 1500$ ,  $K_{c,i}$  decreased with an increase  $R_t$ . This was because the axial mixing of the dispersed phase in the column was occurred.  $K_{c,i}$  also increased with  $E_b$ .  $K_{c,i}$  of nitrogen compounds was smaller than that of other compounds.

### 3.4.2. Correlation of mass transfer coefficient

In previous work<sup>6)</sup>, the mass transfer within continuous phase was more dominant than within the dispersed phase in the overall mass transfer. The mass transfer coefficient in the continuous phase,  $k_{c,i}$ , was, thus, assumed to be equal to  $K_{c,i}$  and compared with the previous correlations<sup>7,8)</sup>. Thorsen and Terjesen have correlated the continuous phase mass transfer coefficients from the single drop to the continuous phase by using  $N_{Re}$ ,  $N_{Sc}$  and  $N_{Sh}$  as:

$$N_{Sh} = -178 + 3.62 \cdot N_{Re}^{1/2} \cdot N_{Sc}^{1/3}$$

This equation was applied to the mass transfer by the internal circulation of the drop. They confirmed the rigid drop by the addition of surfactants. Garner and Suckling<sup>8)</sup> used solid spheres as dispersed phase drops and obtained the correlation below:

$$N_{Sh} = 2 + 0.95 \cdot N_{Re}^{1/2} \cdot N_{Sc}^{1/3}$$

This was applied to the mass transfer of rigid sphere drop.

Here,  $N_{Re}$ ,  $N_{Sc}$  and  $N_{Sh}$  are expressed as follows;

$$N_{Re} = \rho_c u d_p / \mu_c \quad (3.6)$$

$$N_{Sc} = \mu_c / \rho_c D_i \quad (3.7)$$

$$N_{Sh} = k_{c,i} d_p / D_i \quad (3.8)$$

$u$  is slip velocity in the column and obtained from below equations.

$$u_d = R_t / (\rho_d H) \quad (3.9)$$

$$u_c = E_b / \{\rho_c (1-H)\} \quad (3.10)$$

$$u = u_d + u_c \quad (3.11)$$

The diffusivities of component  $i$  were determined by using Wilke-Chang equation.

$$D_i = 7.4 \times 10^{-8} (\text{BM}_c)^{1/2} T / (\mu_c \nu_i^{0.6}) \quad (3.12)$$

$N_{Sh}$  is plotted versus  $N_{Re}^{1/2} \times N_{Sc}^{1/3}$  in **Fig.10**. In this study,  $N_{Sh}$  increased with increasing  $N_{Re}^{1/2} \times N_{Sc}^{1/3}$ . The results in this study were closer to the correlation by Thorsen and Terjesen than to that by Garner and Suckling. So, it was confirmed that in this separation system of AO the mass transfer occurred by the internal circulation of the dispersed drops.  $N_{Sh}$ s of nitrogen compounds were below the two lines. Meanwhile,  $N_{Sh}$ s of other compounds were above the line of Thorsen and Terjesen. In this work, this system was of multi-components and this should make the mass transfer process more complicated. In this case, it was assumed for the mass transfer to be controlled by the continuous phase and this assumption might not be able to fully explain this situation, causing the  $N_{Sh}$  trend.

## 5. Conclusion

The separation of AO with continuous countercurrent spray column was favorably carried out. The yields,  $Y_i$ , and selectivity,  $\beta_{i/2MN}$ , were about 0.5 and 20 at maximum, respectively. It was confirmed that nitrogen compounds could be selectively separated.

The overall volumetric mass transfer coefficient based on the continuous phase concentration,  $K_{ci} \cdot a$  increased with  $R_t$ . The correlation of the continuous phase mass transfer coefficients approximately corresponded to the equation obtained by Thorsen and Terjesen. The disagreement of the mass transfer coefficient correlation of nitrogen compounds was due to the difference of the range of  $N_{Sc}$ .

## Acknowledgment

AO was provided by JFE Chemical Corporation.

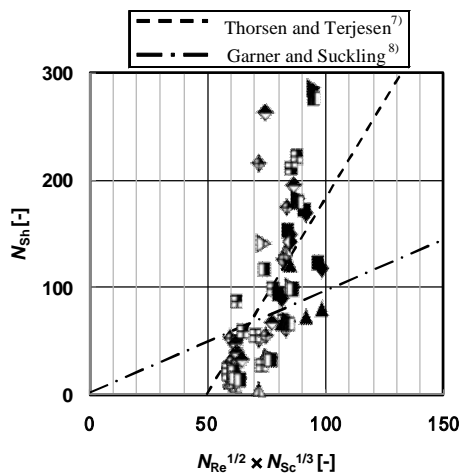


**Fig.10** Correlation of continuous phase mass transfer coefficients (keys are the same as **Fig.6**)

## Nomenclatures

$a$	: specific interfacial area	$[\text{m}^2 \cdot \text{m}^{-3}]$
$B$	: associated factor of solvent	$[-]$
$D$	: diffusivity	$[\text{m}^2 \cdot \text{h}^{-1}]$
$E$	: superficial mass flow rate of continuous phase	$[\text{kg} \cdot \text{m}^{-2} \cdot \text{h}^{-1}]$
$H$	: holdup of dispersed phase	$[-]$
$K_c$	: overall mass transfer coefficient based of continuous phase concentration	$[\text{kg} \cdot \text{m}^{-2} \cdot \text{h}^{-1}]$
$m_i$	: distribution coefficient of component $i$	$[-]$
$M$	: molecular weight	$[\text{kg} \cdot \text{mol}^{-1}]$
$N_{Re}$	: Reynolds number	$[-]$
$N_{Sc}$	: Schmidt number	$[-]$
$N_{Sh}$	: Sherwood number	$[-]$
$R$	: superficial mass flow rate of dispersed phase	$[\text{kg} \cdot \text{m}^{-2} \cdot \text{h}^{-1}]$
$T$	: temperature	$[\text{K}]$
$u$	: velocity of fluids	$[\text{m} \cdot \text{h}^{-1}]$
$\nu$	: molecular volume at standard boiling point	$[\text{m}^3 \cdot \text{mol}^{-1}]$
$x$	: mass fraction in oil phase	$[-]$
$y$	: mass fraction in aqueous phase	$[-]$
$y^*$	: equilibrium mass fraction in aqueous phase	$[-]$
$Y$	: yield	$[-]$
$z$	: distance from top of the column	$[\text{m}]$
$\beta_{i/2MN}$	: separation selectivity of component $i$ relative to 2MN	$[-]$
$\rho$	: density	$[\text{kg} \cdot \text{m}^{-3}]$
$\mu$	: viscosity	$[\text{cP}]$
<Subscripts>		
l	: at equilibrium	
1MN	: 1-methylnaphthalene	
2MN	: 2-methylnaphthalene	
b	: at bottom of the column	
BP	: biphenyl	
DBF	: dibenzofuran	
IL	: indole	
IQ	: isoquinoline	
$i$	: component $i$	
MeOH	: methanol	
N	: naphthalene	
Q	: quinoline	
t	: at top of the column	

## Reference

- 1) Egashira, R., Nagai, M., *Sekiyu Gakkaishi (J. Jpn. Petrol. Inst.)*, **43**, (5), 339 (2000)
- 2) Egashira, R., Salim, C., *Sekiyu Gakkaishi (J. Jpn. Petrol. Inst.)*, **44**, (3), 178 (2001)
- 3) Salim, C., Saito, J., Egashira, R., *Journal of the Japan Petroleum Insititute*, **48**, (1), 60 (2005)
- 4) Salim, C., *Journal of the Japan Petroleum Insititute*, **49**, (6), 326 (2006)
- 5) Egashira, R., *Solv. Ext. Res. Dev. Jpn.*, **14**, 63 (2007)
- 6) Egashira, R., *Journal of the Japan Petroleum Insititute*, **50**, (4), 218 (2007)
- 7) Thorsen and Terjesen, *Chem. Eng. Sci.*, **17**, 137 (1962)
- 8) Garner and Suckling, *Aemr. Inst. Chem. Eng. J.* **4**, 114 (1958)